Multiple-scattering formalism beyond the quasistatic approximation: Analyzing resonances in plasmonic chains

Jakob Rosenkrantz de Lasson, Philip Trøst Kristensen, and Jesper Mørk

Citation: AIP Conf. Proc. **1475**, 158 (2012); doi: 10.1063/1.4750128
View online: http://dx.doi.org/10.1063/1.4750128
View Table of Contents: http://proceedings.aip.org/dbt/dbt.jsp?KEY=APCPCS&Volume=1475&Issue=1
Published by the American Institute of Physics.

Multiple-scattering formalism beyond the quasistatic approximation: Analyzing resonances in plasmonic chains

Jakob Rosenkrantz de Lasson, Philip Trøst Kristensen and Jesper Mørk

DTU Fotonik, Technical University of Denmark, DK-2800 Kongens Lyngby, Denmark

Abstract. We present a multiple-scattering formalism for simulating scattering of electromagnetic waves on spherical inhomogeneities in 3D. The formalism is based on the Lippmann-Schwinger equation and the electromagnetic Green's tensor and applies an expansion of the electric field on spherical wavefunctions. As an example, we analyze localized surface plasmons in chains of Ag spheres, and show how the resonances of such systems depend sensitively on the polarization of the incoming field, the spacing between the particles and the number of particles in the chain.

Keywords: Electromagnetic Green's tensor, scattering, plasmonic nanoparticles, localized surface plasmons
PACS: 02.70.-c, 41.20.-q, 42.25.Fx, 78.20.Bh

INTRODUCTION

Plasmonics has received significant attention in recent years, and diverse applications, including metallic nanoantennas [1], waveguiding beyond the diffraction limit [2] and plasmonic solar cells [3], have been proposed. The possibilities for tailoring the spectra of such systems are intriguing, and at resonance localized surface plasmons (LSPs) give rise to strong field enhancements in the vicinity of the metal particles (see Fig. 1). Consequently, accurate modeling of the electromagnetic field is important, and in particular when particles are closely spaced, modeling of the field beyond the quasistatic approximation is needed [4]. In this context, we present a scattering formalism for modeling optical microstructures and nanosize plasmonic systems, including calculations of the Green's tensor, the Local Density of States (LDOS), Purcell factors and cavity modes [5].

We consider N spherical and non-magnetic scatterers, with permittivities ε_j, embedded in a background medium with permittivity ε_B. The structure is illuminated by the field $\mathbf{E}_\mathrm{B}$, and assuming harmonic time-dependence, $\mathbf{E}(\mathbf{r};t) = \mathbf{E}(\mathbf{r};\omega)\exp(-i\omega t)$, the resulting field is the sum of the incoming field and the scattered field [6]

$$\mathbf{E}(\mathbf{r}) = \mathbf{E}_\mathrm{B}(\mathbf{r}) + \int_V \mathbf{G}_\mathrm{B}(\mathbf{r},\mathbf{r}')k_0^2\Delta\varepsilon(\mathbf{r}')\mathbf{E}(\mathbf{r}')\,\mathrm{d}\mathbf{r}', \qquad (1)$$

with $\mathbf{E}(\mathbf{r}) \equiv \mathbf{E}(\mathbf{r};\omega)$, $k_0 \equiv \omega/c$ and $\Delta\varepsilon(\mathbf{r}) \equiv \varepsilon(\mathbf{r}) - \varepsilon_\mathrm{B}$. V is the volume of the the scatterers, where $\Delta\varepsilon(\mathbf{r}) \neq 0$, and $\mathbf{G}_\mathrm{B}(\mathbf{r},\mathbf{r}')$ is the electromagnetic Green's tensor of the background medium. Eq. (1) is the so-called Lippmann-Schwinger equation which is an implicit equation for the electric field for $\mathbf{r} \in V$; Once it is known in these regions, it is explicit for $\mathbf{r} \notin V$.

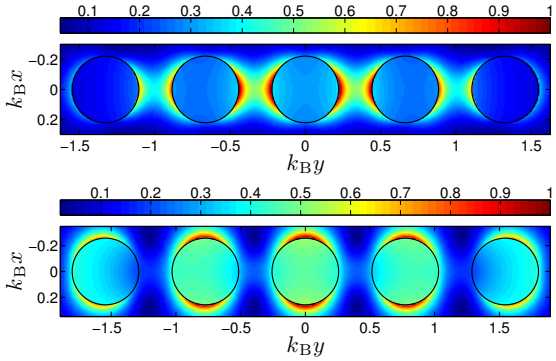

FIGURE 1. Localized surface plasmons around $N = 5$ Ag spheres of radius $R = 10$ nm and spaced a distance $d = R$. Illustrated in $z = 0$-plane. **Top panel:** y-polarization. **Bottom panel:** x-polarization.

The use of the electromagnetic Green's tensor is convenient since the scattered field by construction satisfies the outgoing wave boundary condition in the far-field

$$\mathbf{E}_\mathrm{scat}(\mathbf{r}) \sim \mathbf{f}(\theta,\phi)\frac{\exp(ik_\mathrm{B}r)}{r}, \qquad k_\mathrm{B}r \to \infty, \qquad (2)$$

where $\mathbf{f}(\theta,\phi)$ is the far-field radiation pattern, that is computed analytically in the present formulation.

MULTIPLE-SCATTERING FORMALISM

For solving Eq. (1) we use the general technique of Ref. [7], which we have generalized for 3D problems.

The Fifth International Workshop on Theoretical and Computational Nano-Photonics
AIP Conf. Proc. 1475, 158-160 (2012); doi: 10.1063/1.4750128

We expand the field and the background field inside the jth scatterer, centered at $\mathbf{r}_j^0$, as follows

$$\mathbf{E}(\mathbf{r}) = \sum_\alpha \sum_\nu a_{\nu,\alpha}^j \psi_\nu^j(\mathbf{r}_j)\,\mathbf{e}_\alpha, \tag{3}$$

$$\mathbf{E}_\mathrm{B}(\mathbf{r}) = \sum_\alpha \sum_\nu a_{\nu,\alpha}^{j,\mathrm{B}} \psi_\nu^{j,\mathrm{B}}(\mathbf{r}_j)\,\mathbf{e}_\alpha, \tag{4}$$

with

$$\psi_\nu^j(\mathbf{r}_j) = K_j(\mathbf{r}_j) j_l(k_j r_j) Y_l^m(\theta_j,\phi_j), \tag{5}$$

$$\psi_\nu^{j,\mathrm{B}}(\mathbf{r}_j) = \psi_\nu^j(\mathbf{r}_j)\,(k_j \to k_\mathrm{B}), \tag{6}$$

where $\mathbf{r}_j \equiv \mathbf{r} - \mathbf{r}_j^0$ and $k_j \equiv k_0\sqrt{\varepsilon_j}$. The functions $j_l(x)$ and $Y_l^m(\theta,\phi)$ are the spherical Bessel function of order l and the spherical harmonic of degree l and order m, respectively. $K_j(\mathbf{r}_j)$ contains the normalization of the basis functions and vanishes outside scatterer j, ensuring orthogonality of basis functions of different scatterers. $\nu = \{l,m\}$ is a composite index and $\alpha \in \{x,y,z\}$ is a Cartesian component. Finally, $a_{\nu,\alpha}^j$ are the unknown expansion coefficients, and $a_{\nu,\alpha}^{j,\mathrm{B}}$ are known expansion coefficients of the background field.

Inserting these expansions into Eq. (1), projecting the equation onto $\psi_{\nu'}^{j'}(\mathbf{r}_{j'})\,\mathbf{e}_{\alpha'}$ and summing over all free indices yields a matrix equation for the expansion coefficients

$$\mathbf{a} = \mathbf{M}\mathbf{a}_\mathrm{B} + k_0^2 \mathbf{G}\Delta\varepsilon\mathbf{a}, \tag{7}$$

where $\mathbf{a}$ ($\mathbf{a}_\mathrm{B}$) is a vector containing all $a_{\nu,\alpha}^j$ ($a_{\nu,\alpha}^{j,\mathrm{B}}$). $\mathbf{M}$ is a diagonal matrix, while $\mathbf{G}$ is a non-diagonal matrix. All parts of the formalism are expressed analytically, which prompts high speed in calculations, and rearranging the central Eq. (1) yields an explicit error estimate [7]. This and the direct possibilities for extending to multi-layered geometries [6, 7] makes the formalism viable for modeling, e.g., plasmonic thin-film solar cells.

Scattering objects are commonly characterized by the extinction cross section, C_ext, that may be elegantly computed using the Optical theorem [8]

$$C_\mathrm{ext} = \frac{4\pi}{k_\mathrm{B}} \mathrm{Im}\left(\mathbf{f}(\theta_\mathrm{in},\phi_\mathrm{in}) \cdot \mathbf{e}_\mathrm{in}^*\right), \tag{8}$$

where θ_in and ϕ_in are the spherical angles of the incoming field's wave vector, and $\mathbf{f}(\theta,\phi)$ is given by Eq. (2). $\mathbf{e}_\mathrm{in}$ is the unit polarization vector for the incoming field. It is customary to normalize C_ext to the geometrical cross section, giving the extinction efficiency $Q_\mathrm{ext} \equiv C_\mathrm{ext}/(N\pi R^2)$.

EXAMPLE 1: TWO PARTICLES

We consider two Ag particles (y-direction), of radius $R =$ 10 nm and spaced a distance d. They are embedded in

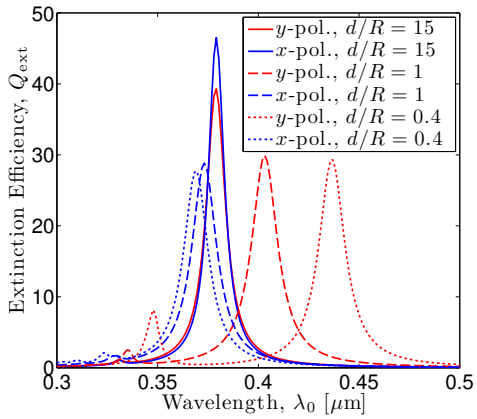

FIGURE 2. Dimer of two Ag spheres, of radius $R = 10$ nm, and spaced the distance d. Extinction efficiency for y- and x-polarization for three values of d/R.

SiO_2 ($\varepsilon_\mathrm{B} = 2.25$), and the permittivity of the Ag spheres is given by the Drude model ($\varepsilon(\omega) = 1 - \omega_\mathrm{p}^2/(\omega^2 + i\gamma\omega)$ with $\omega_\mathrm{p} = 7.9$ eV and $\gamma = 0.06$ eV [9]). We illuminate these by plane waves with an incoming **k**-vector perpendicular (z-direction) to the dimer axis, and polarized along the dimer axis (y-pol.) or perpendicular to the dimer axis (x-pol.).

The extinction spectra are shown for three values of d/R, for the two polarizations, in Fig. 2. The dominant peaks are the dipole resonances, and we observe a redshift and a blueshift for y- and x-polarizations, respectively. To study this more systematically, we plot the resonance wavelengths, λ_0^Res, as function of d/R for the two polarizations in the top panel of Fig. 3. The redshift stems from the induced charges of opposite signs on the spheres in the gap; It acts as a dipole whose potential energy decreases for decreasing d/R [10].

To quantify the dependence of the resonance wavelength under y-polarization, we define the peak shift ratio [10]

$$\Delta\lambda_0^\mathrm{Res} \equiv \frac{\lambda_0^\mathrm{Res} - \lambda_0^\mathrm{single}}{\lambda_0^\mathrm{single}}, \tag{9}$$

where $\lambda_0^\mathrm{single}$ is the resonance wavelength of the isolated Ag sphere. The authors in [10] suggest an exponential increase of $\Delta\lambda_0^\mathrm{Res}$ for decreasing d/R, $\Delta\lambda_0^\mathrm{Res} \sim \exp(-(d/R)/\eta_d)$, η_d being a characteristic interaction length, while a softer dependence on d/R is found in [11], $\Delta\lambda_0^\mathrm{Res} \sim 1/(d/R)$. The latter is explained by the van der Waals force between the spheres that scales inversely with the gap distance.

In the bottom panel of Fig. 3, we show $\Delta\lambda_0^\mathrm{Res}$ as function of $(d/R)^{-1/2}$, and the agreement with the linear fit is acceptable. Similar analyses with two spheres of

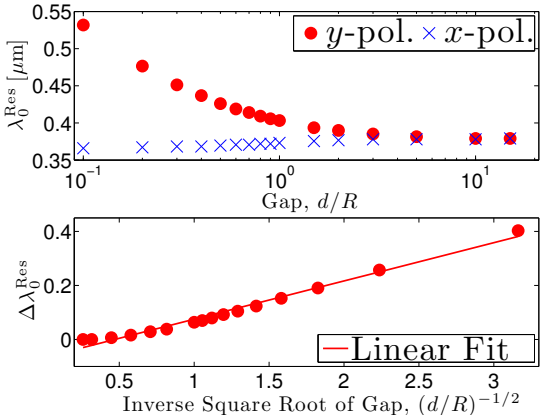

FIGURE 3. Dimer of two Ag spheres, of radius $R = 10$ nm, and spaced the distance d. **Top panel:** Resonance wavelengths in extinction spectra as function of d/R. **Bottom panel:** Peak shift ratio as function of $(d/R)^{-1/2}$.

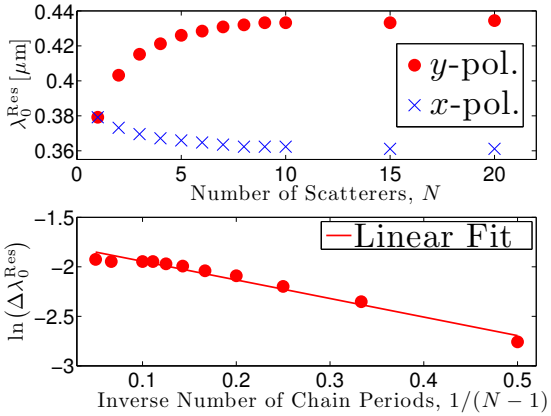

FIGURE 4. Chain of N Ag spheres, of radius $R = 10$ nm, and spaced the distance $d = R$. **Top panel:** Resonance wavelengths as function of N. **Bottom panel:** Logarithm of peak shift ratio as function of inverse number of chain periods, $1/(N-1)$.

radius $R = 25$ nm (not included here) indicate a similar dependence, suggesting a slower increase of the peak shift ratio than reported earlier.

EXAMPLE 2: N PARTICLES

We consider a chain of N Ag spheres, of radius $R = 10$ nm and spaced the distance $d = R$. We vary N and expose them to the y- and x-polarized plane waves described in the previous section. This gives a spectrum for each value of N and for each polarization, and the top panel in Fig. 4 shows the resonance wavelengths as function N.

We observe a clear redshift and a slight blueshift in the y- and x-polarized cases, respectively. For $N = 5$, Fig. 1 shows shows the LSPs in the $z = 0$-plane in the two cases. The induced charges of opposite signs in the gaps in the former case (top panel) give rise to strong field enhancements between the spheres, yielding a redshift as more particles are added. In contrast, for x-polarization (bottom panel) the field is essentially located on the individual particles, with no interaction across the gaps.

In the y-polarized case, an exponential-like convergence to an asymptotic resonance wavelength is observed for increasing N, suggesting that $\Delta\lambda_0^{\text{Res}} \sim \exp(-\eta_N/(N-1))$. The bottom panel of Fig. 4 shows $\ln\left(\Delta\lambda_0^{\text{Res}}\right)$ as function of the inverse number of periods in the chain, $1/(N-1)$. The agreement with the linear fit is not excellent, but acceptable, giving $\eta_N = 1.9$. This suggests an interaction length of approximately two periods in the chain, i.e., each particle interacts with its two nearest neighbors. A similar conclusion is reached in [11].

In conclusion, we have outlined a scheme based on the Lippmann-Schwinger equation and the electromagnetic Green's tensor for simulating, in 3D, scattering of electromagnetic waves on N spheres. The method can be used for calculations of the Green's tensor and the LDOS as well as Purcell factors and cavity modes in optical microstructures (including photonic crystals) and plasmonic nanostructures. We presented two example calculations of the latter, where the resonance wavelengths for chains of Ag nanoparticles were analyzed. We found a strong dependence on the polarization of the incoming field, and a finite interaction length along the chain.

REFERENCES

1. L. Novotny, and N. van Hulst, *Nat. Photon.* **5**, 83–90 (2011).
2. D. K. Gramotnev, and S. I. Bozhevolnyi, *Nat. Photon.* **4**, 83–91 (2010).
3. H. A. Atwater, and A. Polman, *Nat. Mater.* **9**, 205–213 (2010).
4. S. Y. Park, and D. Stroud, *Phys. Rev. B* **69**, 125418 (2004).
5. P. T. Kristensen, C. V. Vlack, and S. Hughes, *Opt. Lett.* **37**, 1649–1651 (2012).
6. L. Novotny, and B. Hecht, *Principles of Nano-Optics*, Cambridge University Press, 2006, first edn.
7. P. T. Kristensen, P. Lodahl, and J. Mørk, *J. Opt. Soc. Am. B* **27**, 228–237 (2010).
8. J. D. Jackson, *Classical Electrodynamics*, Wiley, 1998, third edn.
9. A. F. Koenderink, *Opt. Lett.* **35**, 4208–4210 (2010).
10. P. K. Jain, W. Huang, and M. A. El-Sayed, *Nano Lett.* **7**, 2080–2088 (2007).
11. N. Harris, M. D. Arnold, M. G. Blaber, and M. J. Ford, *J. Phys. Chem. C* **113**, 2784–2791 (2009).